Applied Catalysis B: Environmental 254 (2019) 452–462

Contents lists available at ScienceDirect

Applied Catalysis B: Environmental

journal homepage: www.elsevier.com/locate/apcatb

Construction of a bioinspired laccase-mimicking nanozyme for the degradation and detection of phenolic pollutants

Jinghui Wang[a], Renliang Huang[b,*], Wei Qi[a,c,**], Rongxin Su[a,c], Bernard P. Binks[d,*], Zhimin He[a]

[a] State Key Laboratory of Chemical Engineering, School of Chemical Engineering and Technology, Tianjin University, Tianjin 300072, PR China
[b] Tianjin Key Laboratory of Indoor Air Environmental Quality Control, School of Environmental Science and Engineering, Tianjin University, Tianjin 300072, PR China
[c] Collaborative Innovation Center of Chemical Science and Engineering (Tianjin), Tianjin Key Laboratory of Membrane Science and Desalination Technology, Tianjin University, Tianjin 300072, PR China
[d] Department of Chemistry and Biochemistry, University of Hull, Hull, HU6 7RX, UK

ARTICLE INFO

Keywords:
Nanozyme
Laccase
Peptide
Metal-organic complex
Environmental catalysis

ABSTRACT

Nanozymes, defined as nanomaterials with enzyme-like activity, have attracted extensive interest in both fundamental and applied research. Laccases are members of the multi-copper oxidases, which are utilized as green catalysts in the environmental catalysis and biochemical industry. In this paper, we report a facile strategy for the preparation of a new class of nanozyme (denoted as CH-Cu) with laccase-like activity inspired by the structure of the active site and the electron transfer pathway of laccase *via* the coordination of Cu^{+}/Cu^{2+} with a cysteine (Cys)-histidine (His) dipeptide. The CH-Cu nanozymes exhibit excellent catalytic activity, recyclability and substrate universality and have a similar K_m (Michaelis constant) and a higher v_{max} (maximum rate) than laccase at the same mass concentration. They are robust under a variety of conditions, such as extreme pH, high temperature, long-term storage and high salinity, which can cause severe loss in the catalytic activity of laccase. Higher efficacy of the CH-Cu nanozymes compared with laccase in the degradation of chlorophenols and bisphenols is also demonstrated in a batch reaction. Furthermore, a method for the quantitative detection of epinephrine by a smart phone is established based on the CH-Cu nanozymes. We believe that this nanozyme has promising applications in environmental catalysis and rapid detection and expect that combining key peptides as metal ligands with metal ions to mimic the structure of the catalytic center of a natural enzyme will be a general and important strategy for the design and synthesis of a new type of nanozyme that can be used in various applications.

1. Introduction

Phenolic compounds such as chlorophenols and bisphenols are common toxic pollutants due to their broad use in wood preservatives, pesticides and disinfectants [1]. These phenolic compounds, regarded as threats to human health *via* carcinogenesis, reproductive toxicity, neurotoxicity and endocrine disruption, are widely detected in ground soil and water [2]. Laccases are members of the multi-copper oxidases (MCOs), which catalyze the single-electron oxidation of a wide range of organic substrates, such as polyamines, aryl diamines, *ortho*- and *para*-diphenols as well as polyphenols, with the subsequent four-electron reduction of molecular oxygen to water [3–6]. Therefore, laccases can be utilized as green catalysts in water treatment and soil bioremediation [7,8]. Nevertheless, the poor stability of the laccases in complex environments and the difficulty in recycling laccases severely hamper its practical application due to the high cost. To achieve the recyclability of laccases, many efforts have focused on the immobilization of the laccases on suitable matrices [9–20]. For example, Sarma et al. assembled laccase layer-by-layer on stimuli-responsive membranes for chloro-organic degradation which displayed a loss of 14% of its initial activity after four cycles of operation [14]. Ji et al. immobilized a laccase on a mediator membrane hybrid reactor for the biocatalytic degradation of carbamazepine which maintained 15% of its initial activity after 5 degradation cycles [12]. Recently, Li et al. immobilized a laccase on a Cu_2O nanowire mesocrystal material for the bioremediation of 2,4-dichlorophenol-contaminated water with high biocatalytic activity, and the efficiency remained at 75% after 10 cycles [15]. Although the problem of recyclability was solved by enzyme

* Corresponding authors.
** Corresponding author at: State Key Laboratory of Chemical Engineering, School of Chemical Engineering and Technology, Tianjin University, Tianjin 300072, PR China.
E-mail addresses: tjuhrl@tju.edu.cn (R. Huang), qiwei@tju.edu.cn (W. Qi), b.p.binks@hull.ac.uk (B.P. Binks).

https://doi.org/10.1016/j.apcatb.2019.05.012
Received 30 January 2019; Received in revised form 24 April 2019; Accepted 2 May 2019
Available online 04 May 2019
0926-3373/

immobilization, the stability of the enzymes is still one of the most difficult problems in protein chemistry due to the intrinsic fragility of the enzyme under complex conditions.

To obtain a highly stable biocatalyst, the construction of a nanozyme that mimics the natural enzyme is a promising strategy [21]. Nanozymes, defined as nanomaterials with enzyme-mimicking activity [22], have attracted extensive research interest due to their multifunctionality, low cost and high stability [23]. A variety of nanomaterials and their derivatives, such as noble metals [24–32], metal oxides [32–42] and carbon-based nanomaterials [43–45], were developed as nanozymes in the fields of virus detection [29], the detection of heavy metal ions [46], degradation of organophosphorus-based nerve agents [33] and bacterial inactivation [32,47]. Compared with natural enzymes, nanozymes show better stability and durability due to the inherent properties of the nanomaterial [48,49]. For example, Kuo et al. prepared Au@Cu_2O core@shell nanocrystals as dual-functional catalysts for sustainable environmental applications and the efficiency of methyl orange degradation remained at 89% after 4 cycles [32]. Wang et al. prepared vanadate quantum dots-interspersed g-C_3N_4 nanocomposites for efficient inactivation of *Salmonella* by harvesting visible light [47]. More recently, organic-inorganic hybrids based on the coordination of metal-based nodes with organic ligands have appeared as a promising class of nanozymes owing to their facile preparation, appropriate size and biocompatibility. For example, Liang et al. prepared a nanozyme with laccase-like activity based on guanosine monophosphate (GMP)- coordinated copper [50]. Wang et al. synthesized a porphyrinic metal organic framework PCN-600 (Fe) which is stable under aqueous conditions and has the catalytic activity of peroxidase [51]. Furthermore, this method has been indicated to be effective in mimicking the coordination microenvironment of enzymatic active sites for the design and synthesis of nanozymes with high catalytic activity. Because the structure of the active site and reaction mechanism of peroxidases is well studied [52], a large body of work has focused on the preparation of nanozymes with the catalytic activity of peroxidase [37,51–53]. For instance, Fan et al. optimized the peroxidase-like activity of the Fe_3O_4 nanozyme *via* a single amino acid modification to mimic an enzyme active site [37].

Compared with the research of nanozymes with peroxidase-like activity, there are limited reports on nanozymes with laccase-like activity [50,54,55], which is probably due to the complex structure of the active site and catalytic mechanism of laccase. Specifically, there are four copper sites in laccases that include Type 1 (T1), Type 2 (T2) and binuclear Type 3 (T3) Cu sites. The oxidation of the substrates occurs at the T1 Cu site, and electrons transfer from the T1 Cu site to the T2/T3 trinuclear Cu cluster where the molecular oxygen converts to water through a cysteine-histidine (Cys-His) pathway [5]. Inspired by the structure of the active site and the electron transfer pathway of laccase, we attempted to design and synthesize nanomaterials utilizing a Cys-His dipeptide coordinated with copper ions to mimic this catalytic process.

Herein, we present a facile strategy for the preparation of a new class of nanozyme (denoted as CH-Cu) with laccase-like activity. This strategy is inspired by the structure of the active site and the electron transfer pathway of laccase *via* coordination of Cu^+/Cu^{2+} with a Cys-His dipeptide. Specifically, the CH-Cu nanozymes were synthesized through a hydrothermal method using Cys-His dipeptide and $CuCl_2$ as precursors. The structural characterization of the CH-Cu nanozymes was performed using SEM, FTIR, XPS and XRD. The catalytic activity, stability, recyclability and substrate specificity of the CH-Cu nanozymes were evaluated and compared to the natural enzyme. Additionally, the quantitative detection of epinephrine by a smart phone was established based on the CH-Cu nanozymes. Finally, the catalytic mechanism of action for the CH-Cu nanozymes was proposed.

2. Experimental

2.1. Materials

The cysteine-histidine dipeptide, cysteine and histidine were purchased from GL Biochem (Shanghai) Ltd. 2,4-dichlorophenol (2,4-DP), 4-aminoantipyrine (4-AP), 2,2′-azino- bis(3-ethylbenzothiazoline-6-sulfonic acid) (ABTS), 2-(N-morpholino)ethanesulfonic acid (MES) monohydrate, *N,N*-dimethylformamide (DMF) and copper (II) chloride dihydrate were obtained from Aladdin Industrial Corp. (Shanghai, China). Laccase from *Trametes versicolor* and horseradish peroxidase (HRP) were purchased from Sigma-Aldrich. All other chemicals, such as anhydrous ethanol, sodium chloride, aqueous hydrogen peroxide solution (H_2O_2, 30 wt.%), 4-(1-Hydroxy-2-(methylamino)ethyl)benzene-1,2-diol hydrochloride (epinephrine), phenol, *p*-chlorophenol, 2,6-dimethoxyphenol, hydroquinone, *o*-nitrophenol and *o*-aminophenol, were commercially available and analytical grade. Milli-Q water was used to prepare the solutions and buffers.

2.2. Synthesis of the CH-Cu nanozymes

Aqueous Cys-His dipeptide solution (0.12 M, 2 mL), aqueous copper (II) chloride solution (0.24 M, 1 mL) and 4 mL DMF were mixed in a 15 mL glass pressure tube at 140 °C for 4.5 h. Subsequently, the CH-Cu nanozyme was collected by centrifugation (12,000 rpm, 3 min) and washed with DMF and deionized water three times to remove the excess reactant. Afterwards the obtained CH-Cu nanozymes was dried at 40 °C under vacuum. In addition, we also synthesized Cys-Cu and His-Cu for comparison using cysteine and histidine respectively, following the same procedure as for CH-Cu nanozymes.

2.3. Characterization

Scanning electron microscopy (SEM) images were recorded using a field-emission scanning electron microscope (FESEM, S-4800, Hitachi High-technologies Co., Japan) at an acceleration voltage of 5 kV. All samples were sputter coated with platinum using an E1045 Pt coater (Hitachi High-Technologies Co., Japan) before SEM observation. UV spectroscopy measurements were performed on a dual beam UV spectrophotometer (TU-1900, BPGI, China). X-ray diffraction (XRD) was performed on an X-ray diffractometer (Bruker, Germany) using Cu Kα radiation (λ = 1.5178 Å, 40 kV × 40 mA), and 2θ was scanned from 10° to 85° at 5°/min. X-ray photoelectron spectroscopy (XPS) was carried out on an XPS spectrometer (Kratos Axis Supra) with a monochromatic Al Kα source ($h\nu$ = 1486.6 eV). Zeta potential and dynamic light scattering measurements were performed on a Zetasizer-Nano ZSZEN3600 apparatus (Malvern Instruments, UK). The samples were prepared by dispersing 0.1 mg CH-Cu nanozymes into 1 mL MES buffer with 500 mM NaCl and ethanol, respectively.

2.4. Evaluation of the catalytic performance of CH-Cu nanozymes and laccase

The catalytic activity of the CH-Cu nanozymes and laccase were measured *via* a chromogenic reaction of phenolic compounds with 4-AP. In brief, aqueous solutions of 2,4-DP (1 mg/mL, 100 μL) and 4-AP (1 mg/mL, 100 μL) were mixed with MES buffer (30 mM, pH = 6.8, 700 μL). Then, the CH-Cu aqueous dispersion or laccase solution (1 mg/mL, 100 μL) was added into the mixture. After 1 h of reaction at 25 °C, the reaction mixture was centrifuged (12,000 rpm, 3 min). The absorbance of the supernatant was monitored at 510 nm. To examine the catalytic activity of CH-Cu and laccase for different substrates, aqueous solutions (1 mg/mL, 100 μL) of phenol, *p*-chlorophenol, 2,6-dimethoxyphenol, hydroquinone, *o*-nitrophenol and *o*-aminophenol were measured using the aforementioned method.

2.5. Determination of catalytic kinetic parameters

Various concentrations of 2,4-DP (10, 20, 40, 60, 80 and 100 μg/mL) were reacted with 0.1 mg/mL CH-Cu or laccase and 0.15 mg/mL 4-AP (in excess in all of the reactions) to measure the initial rate of reaction. The kinetic parameters (K_m and v_{max}) were calculated using the Michaelis-Menten Eq. (1):

$$v = (v_{max} \times [S])/(K_m + [S]) \quad (1)$$

where v is the apparent initial catalytic rate, K_m is the apparent Michaelis-Menten constant, v_{max} is the maximum apparent initial reaction rate and $[S]$ is the substrate concentration. In addition, we used the method reported by Jiang et al. [56] to measure k_{cat} of nanozyme or laccase. k_{cat} was calculated using:

$$k_{cat} = v_{max}/[E] \quad (2)$$

where k_{cat} is the rate constant defining the maximum number of substrate molecules converted to product per unit of time and $[E]$ is the molar concentration of nanozyme or laccase.

The molar concentration of nanozyme was calculated by:

$$[E] = \rho_e /(m_s \times N_A) \quad (3)$$

where ρ_e is the mass concentration of nanozyme (g/L), m_s is the mass of a single nanozyme particle (g) and N_A is Avogadro's constant ($6.02 \times 10^{23}\,mol^{-1}$). The mass of a single nanozyme particle was calculated using:

$$m_s = \rho_s \times \pi d^3 \times 10^{-21}/6 \quad (4)$$

where ρ_s is the density of nanozyme (g/cm^3), d is the average diameter of a nanozyme particle (nm) obtained through the statistical analysis of more than 100 nanoparticles in an SEM image.

To measure the density of nanozyme, 100 mg of CH-Cu nanozymes was compressed as a tablet of 10 mm diameter and 0.48 mm height under 14 MPa for 1 min. Subsequently, the volume of the tablet was calculated as 38.06 mm^3 and the mass of tablet was measured again as 91.9 mg. The density of CH-Cu nanozymes was calculated as 2.41 g/cm^3.

2.6. Assessment of catalytic stability

CH-Cu nanozymes or laccase were incubated at various pH (3–9) for 7 h before the evaluation of the catalytic activity to study the effect of pH. The relative activity was compared with the activity at pH = 7. To study the temperature stability of CH-Cu and laccase, they were stored at -18 to 120 °C for 45 min separately before measurement of the catalytic activity. The catalytic activity at 30 °C was taken as reference. The stability during storage was measured every three days for residual catalytic activity of CH-Cu and laccase, which were dispersed in Milli-Q water and stored at 25 °C. Different concentrations of NaCl (0, 150, 300 and 500 mM) were added into the reaction to measure the effect of ionic strength on the catalytic activity. To study the effect of organic solvents on the catalytic activity, various amounts of ethanol (0, 25%, 50%, 70% and 100% v/v) were mixed with the reactants. For these experiments, 1 h was allowed for the chromogenic reaction before monitoring the absorbance of the supernatant at 510 nm.

To evaluate the recyclability of CH-Cu, aqueous solutions of 2,4-DP (1 mg/mL, 100 μL), 4-AP (1 mg/mL, 100 μL), MES buffer (30 mM, pH = 6.8, 700 μL) and CH-Cu (1 mg/mL, 100 μL) were mixed at 25 °C for 1 h per cycle. The CH-Cu, collected by centrifugation (12,000 rpm, 3 min), was washed with Milli-Q water 3 times and re-used for the next reaction cycle.

2.7. Catalytic degradation of phenolic pollutants

2,4-DP (1 mg/mL, 200 μL) and hydroquinone (1 mg/mL, 200 μL) were mixed with MES buffer (30 mM, pH = 6.8, 1400 μL), Milli-Q water (200 μL) and a CH-Cu aqueous dispersion or laccase solution (1 mg/mL, 200 μL). Subsequently, 10 mL/min of oxygen was bubbled into the mixture to degrade the 2,4-DP and hydroquinone. Samples (50 μL) were extracted at different times and centrifuged (12,000 rpm, 3 min) for high-performance liquid chromatography (HPLC) analysis.

The concentration of 2,4-DP, hydroquinone and the final residue were measured by HPLC (Shimadzu, Japan) equipped with a UV–vis detector (SPD-20A, Japan) and a C18 HPLC column (Zorbax SB-C18, 250 mm × 4.6 mm i.d., 5 μm, Agilent, U.S.A.). For HPLC analysis, 70% HPLC-grade methanol and 30% HPLC-grade water (v/v) were used as the mobile phase and the flow rate was set to 0.8 mL/min. Next, 20 μL of the sample was injected and the detection wavelength was set at 226 nm for each analysis. The temperature of the column oven was 40 °C. The samples were filtered by a 0.22 μm filter to remove the insoluble substance before HPLC analysis.

2.8. Oxidation of epinephrine catalyzed by CH-Cu nanozymes and laccase

The CH-Cu aqueous dispersion or laccase solution (1 mg/mL, 100 μL) and 50 μL epinephrine (100 μg/mL) were mixed with MES buffer (50 mM, pH = 6.8, 850 μL) and reacted for 1 h at 25 °C. The oxidation of epinephrine after centrifugation (12,000 rpm, 3 min) was measured at 485 nm. To evaluate the detection limit of epinephrine, different concentrations of epinephrine (5, 10, 20, 30, 40 and 50 μg/mL) were mixed with 0.1 mg/mL of CH-Cu or laccase in the MES buffer for 1 h at 25 °C before the absorbance measurement. The limit of detection was calculated by $3\sigma/b$, where σ is the standard deviation of the blank signals and b is the slope of the regression line.

2.9. Quantitative detection of epinephrine by smart phone

Different concentrations of epinephrine (5, 10, 20, 30, 40, 50 μg/mL) were mixed with 0.1 mg/mL CH-Cu in MES buffer for 1 h at 25 °C. A number of photographs (10) were taken for each concentration of epinephrine from a different site with a varying distance of a flash light. An app (Color Picker Deluxe available on Apple App Store™) was used to recognize the saturation value (saturation is a parameter of HSB color patterns, H: hues, S: saturation and B: brightness) in the color changed regions. The same statistics for the other photographs were performed to find the average of the saturation value for each color changed region. Based on the average saturation value for each color changed region, a standard color-checker and standard curve (correlated to the concentration of epinephrine) were established for rapid visual detection and accurate smart phone detection of epinephrine.

3. Results and discussion

Scheme 1 illustrates the synthesis of the natural laccase-inspired CH-Cu nanozymes. The Cu^{2+} and Cys-His dipeptide, which are the key intermediates of the electron transfer in the natural laccase combination of the substrate oxidation with oxygen reduction [4,6], were used to prepare the nanozyme by a hydrothermal method. The Cys-His dipeptide could be utilized as metal ligands to form a metal-organic framework (MOF) analogy with metal ions because both the thiol group in cysteine and the imidazole group in histidine might contribute to the coordination.

3.1. Structural characterization of CH-Cu nanozymes

As shown in Fig. 1a, CH-Cu is composed of nanoparticles with a diameter ranging from 30 to 80 nm. To further investigate the crystal structure of CH-Cu, XRD characterization was performed. XRD patterns of CH-Cu and the Cys-His dipeptide are shown in Figure S1. The crystal structure of CH-Cu is different from the Cys-His dipeptide and partially ordered between an amorphous and regular crystal structure. This structure might be attributed to the coordination flexibility of the

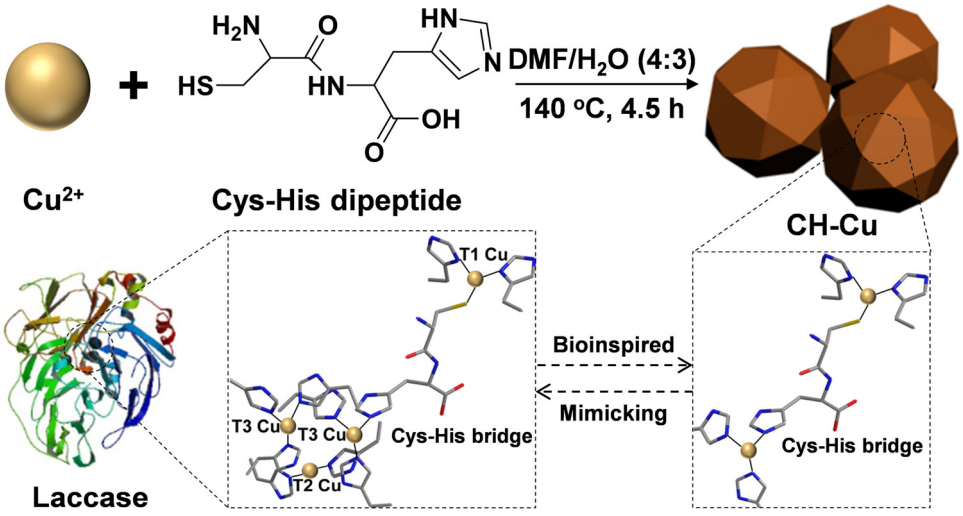

Scheme 1. Schematic illustration of the preparation of laccase mimicking CH-Cu nanozymes, which resembles the catalytic center of natural laccase. PDB code of the laccase is 1V10.

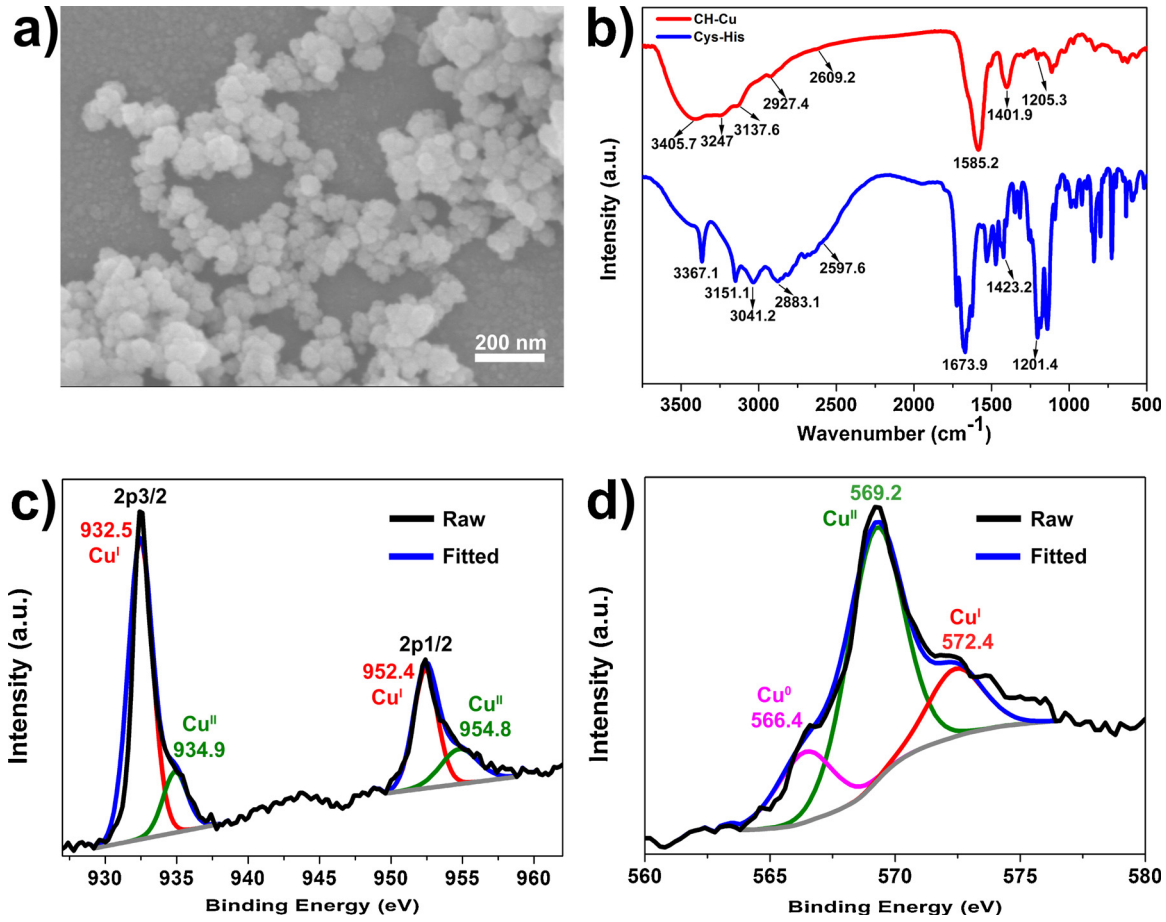

Fig. 1. For CH-Cu nanozymes: (a) SEM image, (b) FTIR spectrum and one for Cys-His dipeptide, (c) Cu 2p XPS spectrum, (d) Cu LMM Auger spectrum. In (c), (d): grey is baseline, green is peaks of Cu^{2+} and red is peaks of Cu^{+}. These peaks were obtained by means of XPS peak-differentiating-imitating analysis.

copper ions and molecular flexibility and asymmetric chemical structure of the Cys-His dipeptide ligand.

To investigate the chemical bonding mechanism in CH-Cu, FTIR spectral analysis of CH-Cu and the Cys-His dipeptide was carried out as shown in Fig. 1b and Table S1. The stretching vibrations at 3406 cm^{-1} and 3367 cm^{-1} in CH-Cu and Cys-His dipeptide, respectively, indicate the existence of an $–NH_2$ group. The peptide bond is demonstrated by a stretching vibration of -NH- at 3247 cm^{-1} and 3151 cm^{-1}, C═O at 1585 cm^{-1} and 1674 cm^{-1} and C–N at 1205 cm^{-1} and 1201 cm^{-1} in the CH-Cu and the Cys-His dipeptide, respectively. Peaks at 2927 cm^{-1} and 2883 cm^{-1}, corresponding to –OH stretching vibration, indicate a carboxyl group in ***CH–Cu*** and Cys-His dipeptide. Absorption from stretching vibrations of a C═N (1402 cm^{-1} and 1423 cm^{-1}) and Cys-His (3138 cm^{-1} and 3041 cm^{-1}) demonstrates the presence of an imidazole

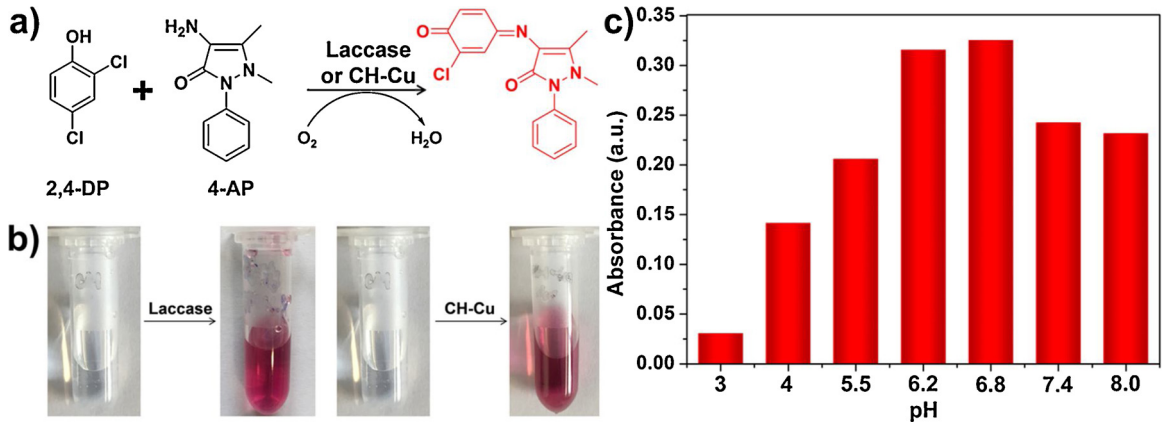

Fig. 2. (a) Reaction of 2,4-DP and 4-AP catalyzed by laccase or CH-Cu, (b) photos of the mixture of 2,4-DP and 4-AP and chromogenic product catalyzed by laccase (left) and CH-Cu (right), (c) pH-dependent activity of CH-Cu nanozymes by detecting absorbance of product at 510 nm.

Table 1
Kinetic parameters of the reaction of 2,4-DP and 4-AP catalyzed by CH-Cu or laccase at 25 °C.

Catalyst	ρ_e (g/L)	[E] (mM)	K_m (mM)	v_{max} (mM min^{-1})	k_{cat} (min^{-1})	k_{cat}/K_m (mM^{-1} min^{-1})
CH-Cu	0.1	3.83×10^{-7}	0.42	7.32×10^{-3}	1.91×10^{4}	4.55×10^{4}
Laccase	0.1	1.55×10^{-3}	0.41	6.41×10^{-3}	4.13	10.07

group in ***CH—Cu*** and Cys-His dipeptide. The -SH stretching vibrations were detected at 2609 cm^{-1} and 2598 cm^{-1}, which exhibits a very weak absorption at approximately 2600 cm^{-1}, confirming the thiol group in CH-Cu and Cys-His dipeptide. The FTIR spectra analysis proves that the dipeptide molecule did not decompose during the synthesis of CH-Cu. It is worth mentioning that the FTIR spectra of CH-Cu are slightly different from that of Cys-His dipeptide, which is likely due to Cu ions binding to the thiol and imidazole groups of Cys-His dipeptide during the synthesis of CH-Cu.

To understand the valence state of copper in CH-Cu, XPS characterization was performed. The full scan spectrum (Figure S2) shows S, C, N, O and Cu elements in CH-Cu, which are consistent with the elements of the Cys-His ligands and copper ions. The content of Cu in the CH-Cu nanozymes is 38.3 wt.% measured by ICP-OES. The molar ratio of Cu and Cys-His dipeptide in CH-Cu nanozymes is approximately 2.5:1. In a high-resolution XPS spectrum (Fig. 1c), peaks at 934.9 eV and 954.8 eV belong to the Cu 2p3/2 and Cu 2p1/2 electrons of Cu^{2+}, respectively. The lower binding energy peaks at 932.5 eV (2p3/2) and 952.4 eV (2p1/2) indicate the existence of Cu^{+}. What is more, approximately 78% of copper in CH-Cu nanozymes is Cu^{+} and the rest (22%) is Cu^{2+}. To gain more insight on the oxidation state of copper in CH-Cu, the Cu LMM Auger spectrum is shown in Fig. 1d. The peak fitting at 572.4 eV suggests the presence of Cu^{+}, the peak fitting at 569.2 eV is attributed to Cu^{2+}. In addition, a few Cu^{0} atoms (pink peak at 566.4 eV in Fig. 1d) were also found in CH-Cu, probably formed *via* the reduction of Cu^{2+}/Cu^{+} by Cys-His dipeptide.

To further investigate the coordination between Cu and S, an S 2p XPS spectrum of CH-Cu nanozymes was recorded. As shown in Figure S3, the peak at 161.6 eV belongs to S-Cu, indicating the existence of coordination between Cu and S (~16% of total S atoms), while the peaks at 163.3 eV indicated that ~59% of thiol groups keep the original chemical state. In addition, S^{0} was also found in the CH-Cu nanozymes, probably formed *via* the oxidation by Cu^{2+}. Because CH-Cu nanozymes have a high content of Cu^{+} (78%), we speculate that the content of S-Cu^{+} should be higher than that of S-Cu^{2+}.

To investigate the effect of the thiol group (cysteine) and the imidazole group (histidine) on the chemical state and coordination of Cu, we prepared Cys-Cu and His-Cu for comparison using cysteine and histidine as ligands, respectively. Cu LMM Auger spectra of Cys-Cu and His-Cu were recorded. As shown in Figure S4, there is Cu^{+} in Cys-Cu, while there is only Cu^{2+} in His-Cu. This data indicates that the existence of the thiol group in cysteine promotes the formation of Cu^{+}.

On the basis of these results, we demonstrate that a large portion of Cu^{2+} was successfully reduced to Cu^{+} owing to the reducibility of the thiol group in the Cys-His dipeptide. Furthermore, we speculate that Cu^{+} mainly binds with the thiol group and Cu^{2+} mainly binds with the imidazole group through a coordinate bond in CH-Cu, which lead to the difference between the FTIR spectra of CH-Cu and Cys-His dipeptide.

3.2. Evaluation of the catalytic performance of CH-Cu nanozymes

The catalytic activity of CH-Cu and laccase were measured *via* a chromogenic reaction of the phenolic compounds with 4-aminoantipyrine (4-AP), as reported previously [50,51]. Specifically, 2,4-DP and 4-AP, which have no absorption at 510 nm (visible region), reacted to generate a product with absorption at 510 nm as shown in Fig. 2b. It is noteworthy that 2,4-DP is the real substrate and that its laccase oxidation product reacts with 4-AP to generate product. The chemical structures of 2,4-DP, 4-AP and product are shown in Fig. 2a.

Because the free Cu^{2+} could catalyze this reaction as well, a contrast experiment was designed as shown in Figure S5. The CH-Cu aqueous dispersion was centrifuged to obtain the supernatant and sediment. After addition of 2,4-DP and 4-AP for 1 h, the supernatant had little activity (light pink), while the sediment had high catalytic activity (dark red). This result confirms the laccase-like catalytic activity derives from the CH-Cu nanoparticles rather than from free Cu^{2+} decomposed from CH-Cu.

Some oxidases, such as glucose oxidase, oxidize substrates *via* the reduction of O_2 to H_2O_2. However, laccase directly reduces O_2 to water without generating H_2O_2. To verify the reduced product of O_2 catalyzed by CH-Cu, a mixture of 2,4-DP and CH-Cu was centrifuged after 1 h of reaction (without 4-AP to avoid the interference of red color). Subsequently, when horseradish peroxidase (HRP) and ABTS were added to the supernatant, no variation of color or absorption was observed (Figure S6 a and b). Afterwards, H_2O_2 was added into the mixture and it turned green immediately, as shown in Figure S6c. These experimental results confirm the absence of H_2O_2. Therefore, CH-Cu is a class of nanozyme with laccase-like activity which does not perform

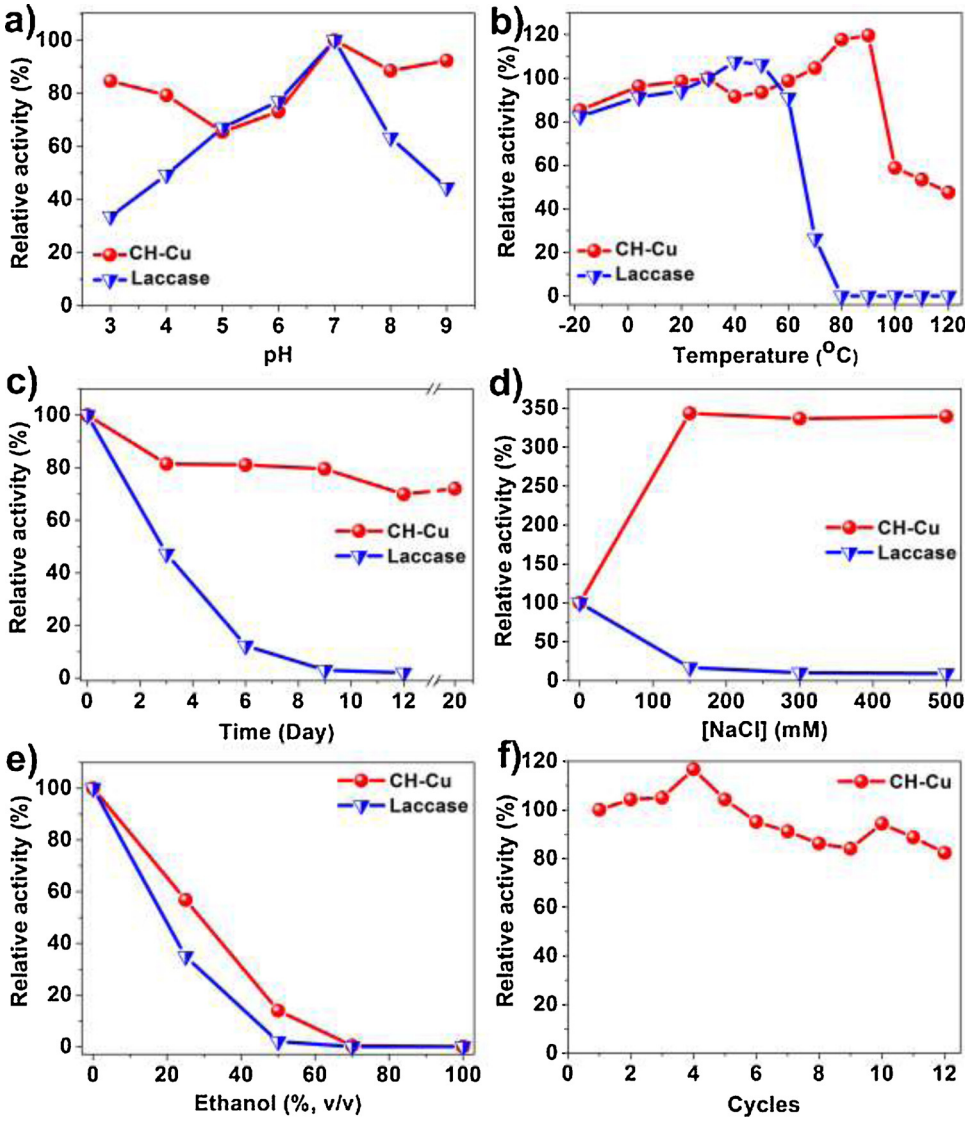

Fig. 3. Stability of CH-Cu and laccase with the same mass concentration at different (a) pH, (b) temperature, (c) storage time, (d) NaCl concentration and (e) content of ethanol. (f) Relative activity of CH-Cu in the chromogenic reaction during the recycling and reuse process. The condition for recycling experiments: 0.1 mg/mL 2,4-DP, 0.1 mg/mL 4-AP, 0.1 mg/mL CH-Cu, pH 6.8, 25 °C, 1 h.

like other oxidases.

The catalytic activity of CH-Cu at different pH values was measured. As shown in Fig. 2c, ***CH—Cu*** has the highest catalytic activity at pH = 6.8 and laccase also has good catalytic activity at this pH. Therefore, pH 6.8 MES buffer was utilized in subsequent catalytic reactions and the catalytic activity of laccase was also measured as contrast.

To study the catalytic kinetic characteristics of CH-Cu, the reaction kinetic parameters of ***CH—Cu*** and laccase were measured at different concentrations of the substrate. Values of K_m and v_{max} were obtained by the Michaelis-Menten model. As shown in Table 1, K_m of ***CH—Cu*** and laccase are almost identical, revealing the equal substrate affinity for them. v_{max} of CH-Cu is slightly higher than that of laccase. These catalytic kinetic parameters prove that the CH-Cu nanozymes constructed by metal ions and key peptides to mimic the structure of the enzymatic catalytic center has similar catalytic activity as laccase. In addition, the active unit of the CH-Cu nanozymes was measured, as shown in Table S2. Compared with previous research, such as copper-containing carbon dots [54] and guanosine monophosphate (GMP) coordinated copper [50], the CH-Cu nanozymes in this work shows higher catalytic activity.

Although CH-Cu nanozymes have similar K_m and v_{max} values to laccase, k_{cat} ($1.91 \times 10^4\ min^{-1}$) and k_{cat}/K_m ($4.55 \times 10^4\ mM^{-1}\ min^{-1}$) of CH-Cu nanozymes are much higher than that of laccase, indicating the higher turnover number and catalytic efficiency of a single CH-Cu nanozyme particle, which has a larger number of active sites than a laccase molecule. A similar result was also found in the case of Fe_3O_4 nanoparticles with peroxidase-mimicking activity (k_{cat} = $3.1 \times 10^5\ s^{-1}$) [56].

In addition, we measured the catalytic activity of laccase and CH-Cu nanozymes with the same amount of Cu atoms. The amount of copper in laccase is 0.32 wt.% and that in ***CH—Cu*** nanozymes is 38.3 wt.%. As a result, the weight ratio of laccase to nanozyme was 120:1 for the activity test. As shown in Figure S7, the relative activity of CH-Cu nanozymes is 26.8% of laccase. Therefore, CH-Cu nanozymes show good laccase-like catalytic activity by increasing the number of active sites in a single particle.

3.3. Catalytic stability and recyclability of CH-Cu nanozymes

High stability and recyclability of the enzyme are both required in practical applications [57]. Hence, enzymes are immobilized on a

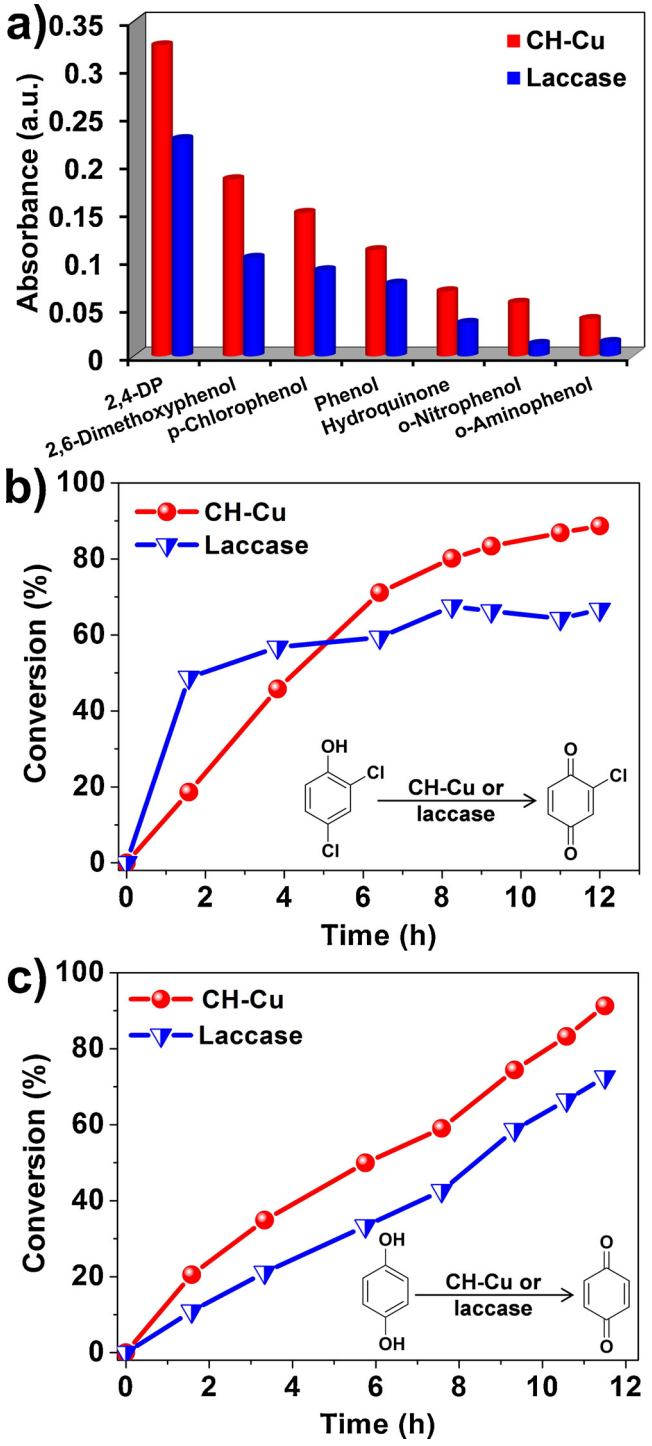

Fig. 4. (a) Catalytic efficiency of CH-Cu and laccase for different substrates and degradation efficiency of CH-Cu and laccase for (b) 2,4-DP and (c) hydroquinone.

matrix to enhance the stability and recyclability [58,59]. For example, Ge et al. immobilized various enzymes on hybrid organic-inorganic nanoflowers to increase the enzymatic stability compared with the free enzyme [58]. Nanozymes are defined as nanomaterials with enzyme-like characteristics [22] and have intrinsically high stability and recyclability. After determining the catalytic activity for the ***CH—Cu*** nanozymes, the stability of the nanozyme at different pH, temperature, storage time, ionic strength, presence of ethanol and the recyclability of CH-Cu were measured.

Specifically, ***CH—Cu*** and laccase were dispersed in different buffers ranging from pH 3.0 to 9.0 at 25 °C for 7 h. Afterwards, the catalytic activities in a pH 6.8 buffer at 25 °C for 1 h were assayed. As shown in Fig. 3a, laccase lost approximately 70% of its catalytic activity after incubation in a pH 3.0 and 9.0 buffer, while the CH-Cu nanozymes maintained at least 60% of its catalytic activity (pH 5.0) and 80%–90% catalytic activity in harsh pH conditions (pH 3.0 and 9.0).

The thermal stability of ***CH—Cu*** was studied next. After incubation at different temperatures ranging from -18 to 120 °C for 45 min, the catalytic activity of laccase decreased gradually and was completely lost at 80 °C (Fig. 3b). However, CH-Cu nanozymes shows good thermal stability from -18 to 90 °C. When incubated at 100 °C for 45 min, the catalytic activity of ***CH—Cu*** nanozymes falls drastically to 58.8%, indicating the decline of chemical stability of ***CH—Cu*** nanozymes beyond 100 °C.

As shown in Fig. 3c, the catalytic activity of laccase decreased gradually with storage in water at 25 °C and became completely inactivated in the 9th day. However, the CH-Cu nanozymes retained 72% of catalytic activity during storage in water at 25 °C for 20 days. In addition, as shown in Figure S8, when the CH-Cu nanozymes were stored in air at room temperature for 210 days, 82% of the original catalytic activity remained. These results indicate that CH-Cu nanozymes show good stability during storage either in air or in water.

Laccase is usually utilized as an environmental catalyst in practical water treatment [4]. Therefore, the influence of ionic strength on activity was studied. As shown in Fig. 3d, upon increasing concentration of NaCl, the catalytic activity of laccase decreased drastically because high ionic strength influenced the charge distribution and spatial structure of the enzyme and reduced its solubility (salting-out effect) causing severe loss of catalytic activity. What is more, chloride ions are a kind of inhibitor of laccase binding to the type 2/type 3 (T2/T3) trinuclear copper site, leading to inactivation of laccase [60]. However, it was surprising that the catalytic activity of CH-Cu increased to 350% with 150, 300 and 500 mM NaCl. To illustrate the role of NaCl, we measured the adsorption of substrate on CH-Cu nanozymes in the absence and presence of NaCl. Specifically, the same amount of 2,4-DP was dissolved in water, CH-Cu aqueous dispersion (1 mg/mL) or CH-Cu aqueous dispersion (1 mg/mL) containing 4 M NaCl. After incubation at 25 °C for 5 h, the supernatant was collected after centrifugation for UV–vis measurement at 284 nm. As shown in Figure S9, the absorbance of 2,4-DP in CH-Cu dispersion is equal to that of 2,4-DP in water, while the value for CH-Cu dispersion containing NaCl is only 62% of that in the absence of NaCl, indicating that approximately 38% of 2,4-DP is adsorbed on the CH-Cu nanozymes in the presence of NaCl. The results demonstrate that the existence of NaCl promotes the adsorption of 2,4-DP on CH-Cu nanozymes and thus enhances the catalytic performance. Furthermore, as shown in Table S3, the zeta potential of CH-Cu increased from -0.72 mV to -2.56 mV with addition of NaCl, and the average 'particle' diameter decreased simultaneously from 824 nm to 665 nm. The increased charge and decreased size of the CH-Cu derived from the addition of NaCl may also contribute to the enhancement of catalytic activity of CH-Cu nanozymes.

To investigate the effect of solvent on the catalytic activity, various amounts of ethanol (0, 25%, 50%, 70% and 100% v/v) were mixed with the reactants. As Fig. 3e shows, the catalytic activity of CH-Cu and laccase decreased upon increasing the content of ethanol. At 100% ethanol, both CH-Cu and laccase were completely inactivated. Subsequently, oxygen was bubbled into the reaction mixture and no catalytic activity of CH-Cu and laccase was observed, indicating that it is the ethanol solvent rather than the absence of oxygen that hinders the reaction.

To evaluate the recyclability of the CH-Cu nanozymes, 2,4-DP and 4-AP were mixed with CH-Cu nanozymes in an MES buffer at 25 °C after 1 h for each cycle. The CH-Cu nanozymes was collected by centrifugation, washed with Milli-Q water and re-used for the next reaction cycle. As shown in Fig. 3f, the CH-Cu nanozymes maintained 82% of its

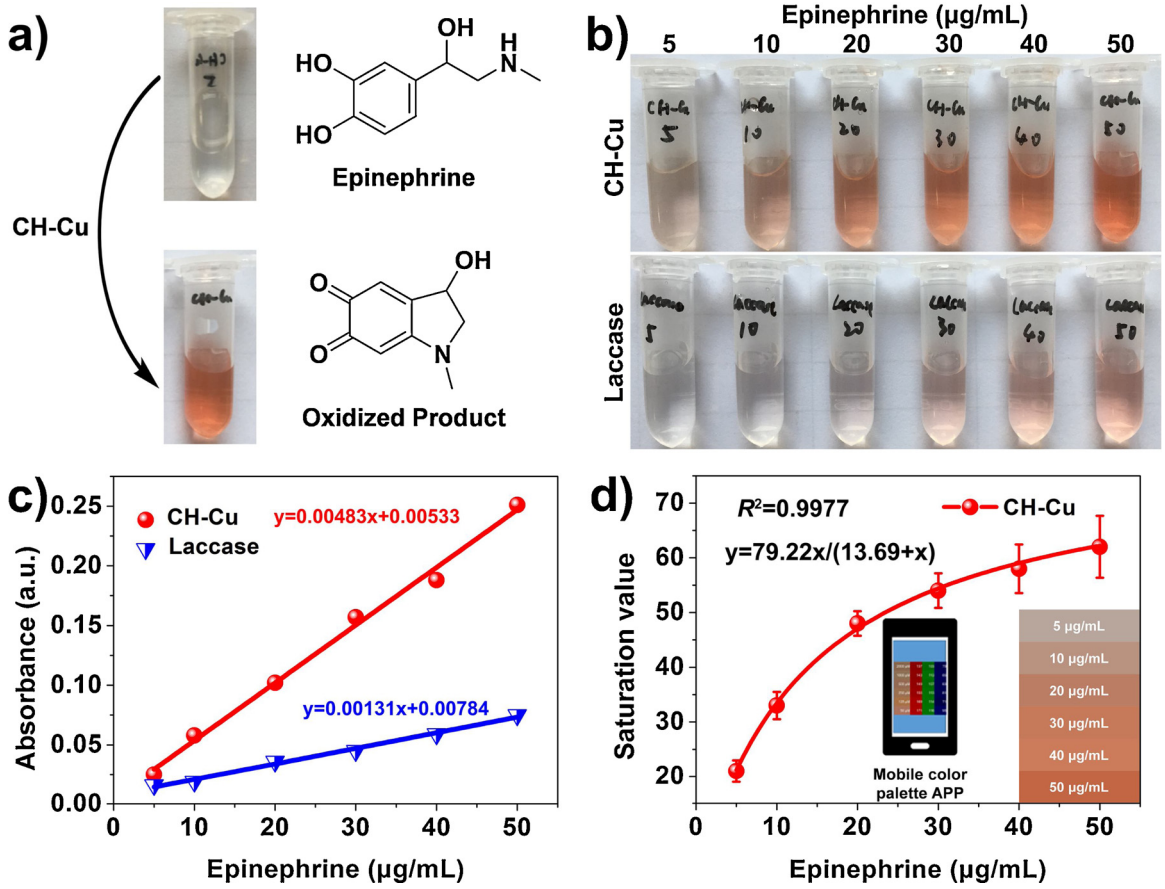

Fig. 5. (a) Photos of epinephrine and its oxidized product catalyzed by CH-Cu for 1 h, (b) photo' of the catalytic activity of CH-Cu and laccase at different concentrations of epinephrine after 1 h reaction, (c) absorbance at 485 nm *versus* concentration of epinephrine catalyzed by CH-Cu or laccase for 1 h, (d) accurate smart phone detection of epinephrine concentration by the standard curve of the saturation value from photos at different concentrations of epinephrine catalyzed by CH-Cu for 1 h. Inset: visual rapid detection of epinephrine by a standard color checker derived from photos for different epinephrine concentrations catalyzed by CH-Cu for 1 h.

Table 2
Kinetic parameters of CH-Cu nanozymes and laccase for oxidizing epinephrine at 25 °C.

Catalyst	ρ_e (g/L)	[*E*] (mM)	K_m (mM)	v_{max} (mM min^{-1})	k_{cat} (min^{-1})	k_{cat}/K_m (mM^{-1} min^{-1})
CH-Cu	0.1	3.83×10^{-7}	0.58	2.74×10^{-2}	7.15×10^{4}	1.23×10^{5}
Laccase	0.1	1.55×10^{-3}	0.16	3.10×10^{-3}	2	12.73

relative activity after twelve cycles while laccase is unable to be recycled. Compared with laccase, the CH-Cu nanozymes show higher catalytic stability and recyclability.

3.4. Catalytic degradation of phenolic pollutants by CH-Cu nanozymes

Laccase is a member of the multi-copper oxidases (MCOs) capable of oxidizing a series of substrates [3]. To measure the substrate universality of the CH-Cu nanozymes, CH-Cu was mixed with various phenolic substances and a chromogenic agent (4-AP). The molecular structures of these phenolic compounds are shown in Figure S10. As shown in Fig. 4a, CH-Cu not only could catalyze the oxidation of these phenolic substances but also shows higher catalytic activities than that of laccase, indicating the favorable substrate universality of CH-Cu nanozymes.

These phenolic substances are significant industrial chemicals and regarded as a category of eco-environmental pollutants. To further investigate the degradation of these pollutants by the CH-Cu nanozymes, 2,4-DP and hydroquinone were chosen as the model substrates of the chlorophenols and bisphenols, respectively. As shown in Fig. 4b, laccase has a higher initial rate of reaction because of its higher substrate affinity, while the CH-Cu nanozymes shows higher degradation efficiency of 2,4-DP. The HPLC chromatograms of 2,4-DP degraded by the CH-Cu nanozymes are shown in Figure S10. The concentration of 2,4-DP decreased during the process of degradation and the benzoquinone product has no absorption at 226 nm (Figure S11). In the case of hydroquinone, CH-Cu nanozymes also show higher degradation efficiency (Fig. 4c). Therefore, the CH-Cu nanozymes have the capability to degrade chlorophenol and bisphenol pollutants and exhibit higher degradation efficiency compared with laccase.

3.5. Detection of epinephrine based on CH-Cu nanozymes

To further develop the environmental applications of CH-Cu nanozymes, epinephrine - a type of catecholamine - was used as a model. Epinephrine is the hormone produced by the adrenal medulla when experiencing an external stimulus and is utilized as a medication to treat arrhythmia, anaphylactic shock and bronchial asthma. Therefore, the quantitative detection of epinephrine is essential for disease diagnosis and pharmaceutical analysis. The CH-Cu nanozymes and laccase

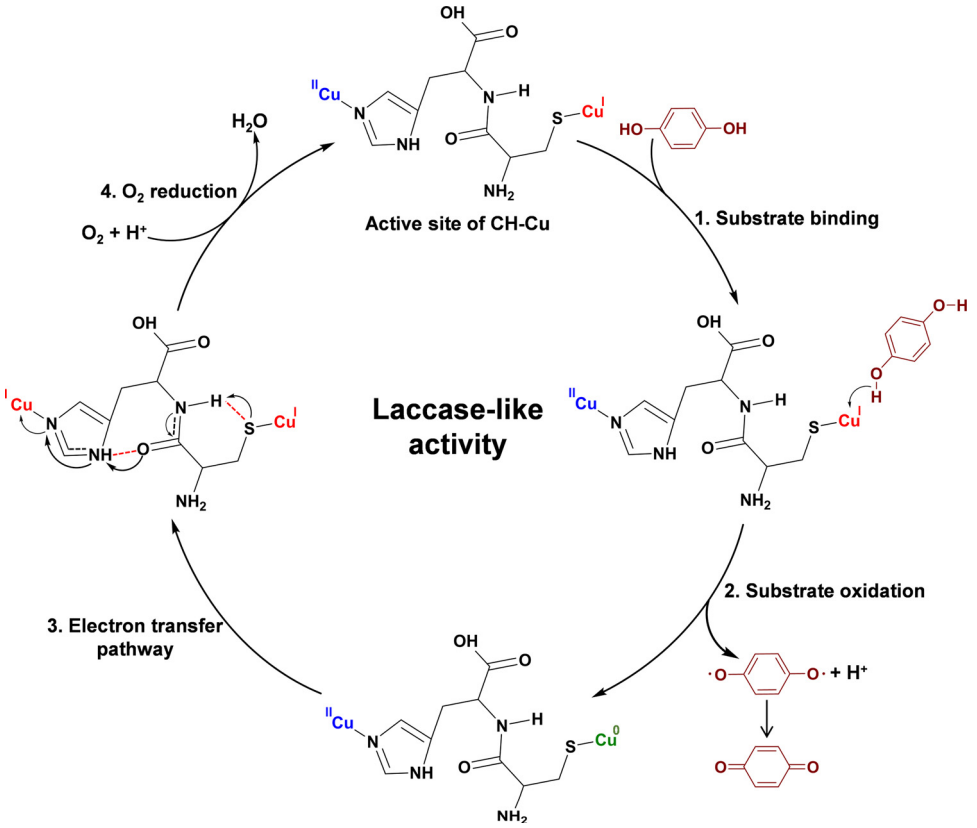

Fig. 6. Schematic of possible catalytic mechanism involving the CH-Cu nanozymes (black dotted lines indicate through-space interactions and red dotted lines indicate H-bonds).

are able to catalyze the oxidation of epinephrine, generating a colored oxidized product (Fig. 5a). Different concentrations of epinephrine (5–50 μg/mL) were mixed with CH-Cu and laccase, and the oxidized product was measured at 485 nm. The reaction kinetic parameters were obtained by the Michaelis-Menten model (Figure S12 and S13). As shown in Table 2, K_m of laccase is lower than that of CH-Cu, indicating higher substrate affinity due to its flexible structure compared with the rigid structure of the CH-Cu nanozymes. However, v_{max} of CH-Cu is much higher (9 times) than that of laccase, which is likely attributable to the pair of multivalent copper ions and the dipeptide Cys-His, a critical electron transfer intermediate in laccase. In addition, the much higher k_{cat} and k_{cat}/K_m values of CH-Cu were also obtained using epinephrine as substrate compared to laccase.

The colored oxidized product of epinephrine could be utilized as a method for epinephrine detection (Fig. 5b-d). As shown in Fig. 5c, the absorbance of the colored oxidized product at 485 nm increased as a function of epinephrine concentration catalyzed by equal amounts of CH-Cu nanozymes or laccase. Because of the higher catalytic activity of the CH-Cu nanozymes, the detection limit of epinephrine (0.31 μg/mL) is lower than that catalyzed by laccase (1.15 μg/mL). Hence, the method involving CH-Cu nanozymes is more sensitive than with laccase.

Since the colored oxidized product of epinephrine is in the visible region, we designed a standard color checker for visual rapid detection of epinephrine catalyzed by CH-Cu (inset of Fig. 5d), and a standard curve for accurate smart phone detection of epinephrine as shown in Fig. 5d. Specifically, after 1 h of reaction with the CH-Cu nanozymes, the mixture was filtered to obtain the supernatant. Then, the saturation of the sample detected by a smart phone *via* the Mobile Color Palette App was placed into the standard curve (Fig. 5d) to obtain the concentration of epinephrine. Saturation is a parameter of HSB color patterns, H: hues, S: saturation and B: brightness. Therefore, a rapid, convenient and precise method for the determination of epinephrine concentration was established based on our CH-Cu nanozymes.

3.6. Catalytic mechanism involving CH-Cu nanozymes

For natural laccase, Solomon and co-workers proposed a clear catalytic mechanism [5,61]. Specifically, substrate is bound to the active center and further oxidized near the T1 Cu, and electrons are transferred *via* the Cys-His pathway to the T2/T3 trinuclear copper cluster (TNC) where dioxygen reduction occurs. As reported previously, the Cys-His pathway contains two potential electron-transfer routes: P1 through the protein backbone and P2 through the H-bond between Cys and His [61]. To investigate the role of Cys-His dipeptide in CH-Cu nanozymes, we prepared Cys-Cu and His-Cu for comparison using cysteine and histidine instead of Cys-His dipeptide, respectively. The activity of CH-Cu, Cys-Cu, His-Cu is summarized in Figure S14. As mentioned before, His-Cu has no Cu^+ and exhibited little catalytic activity, while Cys-Cu has both Cu^+ and Cu^{2+} but its activity is much lower than that of CH-Cu. The results suggest that Cu^+/Cu^{2+} together with Cys-His dipeptides contribute to the high catalytic activity of CH-Cu. As we know, Cys-His is an electron transfer bridge in natural laccase. The redox potential of Cu^+/Cu^0 is higher than Cu^{2+}/Cu^+, so the electron transfer probably occurs from Cu^+ to Cu^{2+} *via* the Cys-His pathway, which was proven in natural laccase. Therefore, we propose that Cu^+ mainly binds with the thiol group and Cu^{2+} mainly binds with the imidazole group through a coordinate bond in CH-Cu nanozymes.

Inspired by the catalytic mechanism of natural laccase, we propose a possible catalytic mechanism of CH-Cu nanozymes shown in Fig. 6, including (i) substrate binding, (ii) substrate oxidation near the Cu-S site, (iii) electron transfer *via* Cys-His pathway and (iv) O_2 reduction near the Cu-N site. To illustrate the catalytic mechanism, the active site of the CH-Cu nanozymes was simplified to: Cu^I binds to the thiol group through chemical binding owing to the reducibility of –SH (from Cys) and Cu^{II} binds to the imidazole group (from His) through a coordination

bond. Since the oxidation ability of Cu^{I} is higher than that of Cu^{II}, phenolic substrates are oxidized to benzoquinone by Cu^{I} which is the primary electron acceptor site with single-electron oxidation in the CH-Cu nanozymes. The electrons are transferred through the Cys-His pathway to Cu^{II}. Specifically, the highly covalent Cu^{I}-S (from Cys) bond is in favor of the rapid electron transfer. This electron transfer pathway consists of several covalent bonds, H-bonds and through-space interactions (saturated bonds). Subsequently, Cu^{II} converts to Cu^{I} after obtaining electrons. Owing to the lack of protection of the surrounding chemical groups, Cu^{I} is oxidized to Cu^{II} by oxygen in the system, which is the final electron acceptor *via* a four-electron reduction of molecular oxygen to water. Finally, the CH-Cu nanozyme is regenerated by Cu^{I} oxidation.

4. Conclusions

In summary, we have successfully prepared a new CH-Cu nanozyme inspired by the structure of the laccase active site. Compared with laccase, the CH-Cu nanozymes shows higher catalytic activity under normal conditions and greater stability at extreme pH, temperature, after long-term storage and at high salt concentration. The CH-Cu nanozymes also display good recyclability. Acceptable substrate universality was observed in the CH-Cu nanozymes, enabling us to utilize it for chlorophenol and bisphenol degradation and the quantitative detection of epinephrine. Furthermore, the catalytic mechanism involving the CH-Cu nanozymes was proposed. The relatively low cost, high catalytic activity, excellent stability, recyclability and substrate universality demonstrate its promising application in environmental catalysis and rapid detection. Moreover, in view of the versatile coordination characteristics of peptides with metal ions, our results provide a general method for combining key peptides as metal ligands with metal ions to mimic the structure of the catalytic center of a natural enzyme. Therefore, we believe that this new concept and method could be developed for the design and synthesis of a new type of nanozyme for various applications.

Acknowledgments

This work was supported by the National Natural Science Foundation of China (Nos. 21621004, 51773149 and 21777112).

Appendix A. Supplementary data

Supplementary data associated with this article can be found, in the online version, at https://doi.org/10.1016/j.apcatb.2019.05.012.

References

[1] C. Barrios-Estrada, M. de Jesus Rostro-Alanis, B.D. Munoz-Gutierrez, H.M.N. Iqbal, S. Kannan, R. Parra-Saldivar, Emergent contaminants: endocrine disruptors and their laccase-assisted degradation - a review, Sci. Total Environ. 612 (2018) 1516–1531.
[2] E. Torres, I. Bustos-Jaimes, S. Le Borgne, Potential use of oxidative enzymes for the detoxification of organic pollutants, Appl. Catal. B Environ. 46 (2003) 1–15.
[3] O. Farver, S. Wherland, O. Koroleva, D.S. Loginov, I. Pecht, Intramolecular electron transfer in laccases, FEBS J. 278 (2011) 3463–3471.
[4] P. Giardina, V. Faraco, C. Pezzella, A. Piscitelli, S. Vanhulle, G. Sannia, Laccases: a never-ending story, Cell. Mol. Life Sci. 67 (2010) 369–385.
[5] S.M. Jones, E.I. Solomon, Electron transfer and reaction mechanism of laccases, Cell. Mol. Life Sci. 72 (2015) 869–883.
[6] S. Riva, Laccases: blue enzymes for green chemistry, Trends Biotechnol. 24 (2006) 219–226.
[7] P. Peralta-Zamora, C.M. Pereira, E.R.L. Tiburtius, S.G. Moraes, M.A. Rosa, R.C. Minussi, N. Durán, Decolorization of reactive dyes by immobilized laccase, Appl. Catal. B Environ. 42 (2003) 131–144.
[8] N. Diano, V. Grano, L. Fraconte, P. Caputo, A. Ricupito, A. Attanasio, M. Bianco, U. Bencivenga, S. Rossi, I. Manco, Non-isothermal bioreactors in enzymatic remediation of waters polluted by endocrine disruptors: BPA as a model of pollutant, Appl. Catal. B Environ. 69 (2007) 252–261.
[9] X. Cao, J. Luo, J.M. Woodley, Y. Wan, Bioinspired multifunctional membrane for aquatic micropollutants removal, ACS Appl. Mater. Interfaces 8 (2016) 30511–30522.
[10] J. Hou, G. Dong, B. Luu, R.G. Sengpiel, Y. Ye, M. Wessling, V. Chen, Hybrid membrane with TiO2 based bio-catalytic nanoparticle suspension system for the degradation of bisphenol-A, Bioresour. Technol. 169 (2014) 475–483.
[11] J. Hou, G. Dong, Y. Ye, V. Chen, Laccase immobilization on titania nanoparticles and titania-functionalized membranes, J. Membr. Sci. 452 (2014) 229–240.
[12] C. Ji, J. Hou, K. Wang, Y. Zhang, V. Chen, Biocatalytic degradation of carbamazepine with immobilized laccase-mediator membrane hybrid reactor, J. Membr. Sci. 502 (2016) 11–20.
[13] S. Li, J. Luo, Y. Wan, Regenerable biocatalytic nanofiltration membrane for aquatic micropollutants removal, J. Membr. Sci. 549 (2018) 120–128.
[14] R. Sarma, M.S. Islam, A.F. Miller, D. Bhattacharyya, Layer-by-layer-assembled laccase enzyme on stimuli-responsive membranes for chloro-organics degradation, ACS Appl. Mater. Interfaces 9 (2017) 14858–14867.
[15] G. Li, P. Ma, Y. He, Y. Zhang, Y. Luo, C. Zhang, H. Fan, Enzyme-nanowire mesocrystal hybrid materials with an extremely high biocatalytic activity, Nano Lett. 18 (2018) 5919–5926.
[16] J.B. Costa, M.J. Lima, M.J. Sampaio, M.C. Neves, J.L. Faria, S. Morales-Torres, A.P.M. Tavares, C.G. Silva, Enhanced biocatalytic sustainability of laccase by immobilization on functionalized carbon nanotubes/polysulfone membranes, Chem. Eng. J. 355 (2019) 974–985.
[17] X. Jiang, Y. Yu, X. Li, X.Z. Kong, High yield preparation of uniform polyurea microspheres through precipitation polymerization and their application as laccase immobilization support, Chem. Eng. J. 328 (2017) 1043–1050.
[18] L. Lonappan, Y. Liu, T. Rouissi, F. Pourcel, S.K. Brar, M. Verma, R.Y. Surampalli, Covalent immobilization of laccase on citric acid functionalized micro-biochars derived from different feedstock and removal of diclofenac, Chem. Eng. J. 351 (2018) 985–994.
[19] R. Xu, J. Cui, R. Tang, F. Li, B. Zhang, Removal of 2,4,6-trichlorophenol by laccase immobilized on nano-copper incorporated electrospun fibrous membrane-high efficiency, stability and reusability, Chem. Eng. J. 326 (2017) 647–655.
[20] D. Wu, Q. Feng, T. Xu, A. Wei, H. Fong, Electrospun blend nanofiber membrane consisting of polyurethane, amidoxime polyarcylonitrile, and β-cyclodextrin as high-performance carrier/support for efficient and reusable immobilization of laccase, Chem. Eng. J. 331 (2018) 517–526.
[21] J. Wu, X. Wang, Q. Wang, Z. Lou, S. Li, Y. Zhu, L. Qin, H. Wei, Nanomaterials with enzyme-like characteristics (nanozymes): next-generation artificial enzymes (II), Chem. Soc. Rev. 48 (2019) 1004–1076.
[22] H. Wei, E. Wang, Nanomaterials with enzyme-like characteristics (nanozymes): next-generation artificial enzymes, Chem. Soc. Rev. 42 (2013) 6060–6093.
[23] Y. Lin, J. Ren, X. Qu, Catalytically active nanomaterials: a promising candidate for artificial enzymes, Acc. Chem. Res. 47 (2014) 1097–1105.
[24] W. Luo, C. Zhu, S. Su, D. Li, Y. He, Q. Huang, C. Fan, Self-catalyzed, self-limiting growth of glucose oxidase-mimicking gold nanoparticles, ACS Nano 4 (2010) 7451–7458.
[25] M. Comotti, C. Della Pina, R. Matarrese, M. Rossi, The catalytic activity of naked gold particles, Angew. Chem. Int. Ed 116 (2004) 5936–5939.
[26] M. Comotti, C. Della Pina, E. Falletta, M. Rossi, Aerobic oxidation of glucose with gold catalyst: hydrogen peroxide as intermediate and reagent, Adv. Synth. Catal. 348 (2006) 313–316.
[27] L. Fan, X. Xu, C. Zhu, J. Han, L. Gao, J. Xi, R. Guo, Tumor catalytic-photothermal therapy with yolk-shell gold@carbon nanozymes, ACS Appl. Mater. Interfaces 10 (2018) 4502–4511.
[28] Y. Lin, J. Ren, X. Qu, Nano-gold as artificial enzymes: hidden talents, Adv. Mater 26 (2014) 4200–4217.
[29] S. Oh, J. Kim, V.T. Tran, D.K. Lee, S.R. Ahmed, J.C. Hong, J. Lee, E.Y. Park, J. Lee, Magnetic nanozyme-linked immunosorbent assay for ultrasensitive influenza a virus detection, ACS Appl. Mater. Interfaces 10 (2018) 12534–12543.
[30] J. Wu, K. Qin, D. Yuan, J. Tan, L. Qin, X. Zhang, H. Wei, Rational design of Au@Pt multibranched nanostructures as bifunctional nanozymes, ACS Appl. Mater. Interfaces 10 (2018) 12954–12959.
[31] Y. Zhang, F. Wang, C. Liu, Z. Wang, L. Kang, Y. Huang, K. Dong, J. Ren, X. Qu, Nanozyme decorated metal-organic frameworks for enhanced photodynamic therapy, ACS Nano 12 (2018) 651–661.
[32] M.Y. Kuo, C.F. Hsiao, Y.H. Chiu, T.H. Lai, M.J. Fang, J.Y. Wu, J.W. Chen, C.L. Wu, K.H. Wei, H.C. Lin, Y.J. Hsu, Au@Cu2O core@shell nanocrystals as dual-functional catalysts for sustainable environmental applications, Appl. Catal. B Environ. 242 (2019) 499–506.
[33] A.A. Vernekar, T. Das, G. Mugesh, Vacancy-engineered nanoceria: enzyme mimetic hotspots for the degradation of nerve agents, Angew. Chem. Int. Ed 128 (2016) 1434–1438.
[34] F. Chen, M. Bai, K. Cao, Y. Zhao, J. Wei, Y. Zhao, Fabricating MnO_2 nanozymes as intracellular catalytic DNA circuit generators for versatile imaging of base-excision repair in living cells, Adv. Funct. Mater. 27 (2017) 1702748.
[35] J. Dong, L. Song, J.J. Yin, W. He, Y. Wu, N. Gu, Y. Zhang, Co_3O_4 nanoparticles with multi-enzyme activities and their application in immunohistochemical assay, ACS Appl. Mater. Interfaces 6 (2014) 1959–1970.
[36] H. Fan, G. Yan, Z. Zhao, X. Hu, W. Zhang, H. Liu, X. Fu, T. Fu, X.B. Zhang, W. Tan, A smart photosensitizer-manganese dioxide nanosystem for enhanced photodynamic therapy by reducing glutathione levels in cancer cells, Angew. Chem. Int. Ed 55 (2016) 5477–5482.
[37] K. Fan, H. Wang, J. Xi, Q. Liu, X. Meng, D. Duan, L. Gao, X. Yan, Optimization of Fe_3O_4 nanozyme activity via single amino acid modification mimicking an enzyme active site, Chem. Commun. (Camb.) 53 (2016) 424–427.
[38] S. Ghosh, P. Roy, N. Karmodak, E.D. Jemmis, G. Mugesh, Nanoisozymes: crystal-facet-dependent enzyme-mimetic activity of V_2O_5 nanomaterials, Angew. Chem.

Int. Ed. 57 (2018) 1–7.
[39] Y. Huang, Z. Liu, C. Liu, E. Ju, Y. Zhang, J. Ren, X. Qu, Self-assembly of multi-nanozymes to mimic an intracellular antioxidant defense system, Angew. Chem. Int. Ed. 55 (2016) 6646–6650.
[40] A.A. Vernekar, D. Sinha, S. Srivastava, P.U. Paramasivam, P. D'Silva, G. Mugesh, An antioxidant nanozyme that uncovers the cytoprotective potential of vanadia nanowires, Nat. Commun. 5 (2014) 5301.
[41] L. Gao, J. Zhuang, L. Nie, J. Zhang, Y. Zhang, N. Gu, T. Wang, J. Feng, D. Yang, S. Perrett, X. Yan, Intrinsic peroxidase-like activity of ferromagnetic nanoparticles, Nat. Nanotechnol. 2 (2007) 577–583.
[42] L. Huang, W. Zhang, K. Chen, W. Zhu, X. Liu, R. Wang, X. Zhang, N. Hu, Y. Suo, J. Wang, Facet-selective response of trigger molecule to CeO2 {110} for up-regulating oxidase-like activity, Chem. Eng. J. 330 (2017) 746–752.
[43] K. Fan, J. Xi, L. Fan, P. Wang, C. Zhu, Y. Tang, X. Xu, M. Liang, B. Jiang, X. Yan, L. Gao, In vivo guiding nitrogen-doped carbon nanozyme for tumor catalytic therapy, Nat. Commun. 9 (2018) 1440.
[44] Y. Hu, X.J. Gao, Y. Zhu, F. Muhammad, S. Tan, W. Cao, S. Lin, Z. Jin, X. Gao, H. Wei, Nitrogen-doped carbon nanomaterials as highly active and specific peroxidase mimics, Chem. Mater. 30 (2018) 6431–6439.
[45] Z. Mohammadpour, A. Safavi, M. Shamsipur, A new label free colorimetric chemosensor for detection of mercury ion with tunable dynamic range using carbon nanodots as enzyme mimics, Chem. Eng. J. 255 (2014) 1–7.
[46] L. Huang, Q. Zhu, J. Zhu, L. Luo, S. Pu, W. Zhang, W. Zhu, J. Sun, J. Wang, Portable colorimetric detection of Mercury(II) based on a non-noble metal nanozyme with tunable activity, Inorg. Chem. 58 (2019) 1638–1646.
[47] R. Wang, X. Kong, W. Zhang, W. Zhu, L. Huang, J. Wang, X. Zhang, X. Liu, N. Hu, Y. Suo, J. Wang, Mechanism insight into rapid photocatalytic disinfection of Salmonella based on vanadate QDs-interspersed g-C_3N_4 heterostructures, Appl. Catal. B Environ. 225 (2018) 228–237.
[48] H. Wang, K. Wan, X. Shi, Recent advances in nanozyme research, Adv. Mater. (2018) 1805368.
[49] Y. Huang, J. Ren, X. Qu, Nanozymes: classification, catalytic mechanisms, activity regulation, and applications, Chem. Rev. 119 (2019) 4357–4412.
[50] H. Liang, F. Lin, Z. Zhang, B. Liu, S. Jiang, Q. Yuan, J. Liu, Multicopper laccase mimicking nanozymes with nucleotides as ligands, ACS Appl. Mater. Interfaces 9 (2017) 1352–1360.
[51] K. Wang, D. Feng, T.F. Liu, J. Su, S. Yuan, Y.P. Chen, M. Bosch, X. Zou, H.C. Zhou, A series of highly stable mesoporous metalloporphyrin Fe-MOFs, J. Am. Chem. Soc. 136 (2014) 13983–13986.
[52] Q. Wang, Z. Yang, X. Zhang, X. Xiao, C.K. Chang, B. Xu, A supramolecular-hydrogel-encapsulated hemin as an artificial enzyme to mimic peroxidase, Angew. Chem. Int. Ed 46 (2007) 4285–4289.
[53] P. Zhang, D. Sun, A. Cho, S. Weon, S. Lee, J. Lee, J.W. Han, D.P. Kim, W. Choi, Modified carbon nitride nanozyme as bifunctional glucose oxidase-peroxidase for metal-free bioinspired cascade photocatalysis, Nat. Commun. 10 (2019) 940.
[54] X. Ren, J. Liu, J. Ren, F. Tang, X. Meng, One-pot synthesis of active copper-containing carbon dots with laccase-like activities, Nanoscale 7 (2015) 19641–19646.
[55] Y. Wang, C. He, W. Li, J. Zhang, Y. Fu, Catalytic performance of oligonucleotide-templated Pt nanozyme evaluated by laccase substrates, Catal. Lett. 147 (2017) 2144–2152.
[56] B. Jiang, D. Duan, L. Gao, M. Zhou, K. Fan, Y. Tang, J. Xi, Y. Bi, Z. Tong, G.F. Gao, N. Xie, A. Tang, G. Nie, M. Liang, X. Yan, Standardized assays for determining the catalytic activity and kinetics of peroxidase-like nanozymes, Nat. Protoc. 13 (2018) 1506–1520.
[57] Y. Zhang, J. Ge, Z. Liu, Enhanced activity of immobilized or chemically modified enzymes, ACS Catal. 5 (2015) 4503–4513.
[58] J. Ge, J. Lei, R.N. Zare, Protein-inorganic hybrid nanoflowers, Nat. Nanotechnol. 7 (2012) 428–432.
[59] J. Wang, R. Huang, W. Qi, R. Su, Z. He, Oriented enzyme immobilization at the oil/water interface enhances catalytic activity and recyclability in a pickering emulsion, Langmuir 33 (2017) 12317–12325.
[60] F. Xu, Oxidation of phenols, anilines, and benzenethiols by fungal laccases: correlation between activity and redox potentials as well as halide inhibition, Biochemistry 35 (1996) 7608–7614.
[61] R.G. Hadt, S.I. Gorelsky, E.I. Solomon, Anisotropic covalency contributions to superexchange pathways in type one copper active sites, J. Am. Chem. Soc. 136 (2014) 15034–15045.